Ilari Hänninen and Keijo Nikoskinen, Implementation of method of moments for numerical analysis of corrugated surfaces with impedance boundary condition, IEEE Transactions on Antennas and Propagation, Vol. 56, no. 1, pp. 278-281, 2008.

Therefore, very few sample points are needed for sufficiently good accuracies for near-singular and near-hypersingular kernels of potential integrals. Also, an optimum criterion for the distribution of sample points in two directions was found proportional to the radial and angular dimensions of the instantaneous slices of the source domain.

ACKNOWLEDGMENT

This work was carried out at the Institute of Radio Frequency Technology (IHF), Universität Stuttgart, Stuttgart, Germany under the collaborative Ph.D. scholarship scheme between the Higher Education Commission of Pakistan (HEC) and the Deutscher Akademischer Austausch Dienst (DAAD).

REFERENCES

[1] M. G. Duffy, "Quadrature over a pyramid or cube of integrands with a singularity," *SIAM J. Numer. Anal.*, vol. 19, no. 6, pp. 1260–1262, Dec. 1982.

[2] M. A. Khayat and D. R. Wilton, "Numerical evaluation of singular and near-singular potential integrals," *IEEE Trans. Antennas Propag.*, vol. 53, pp. 3180–3190, Oct. 2005.

[3] P. W. Fink, D. R. Wilton, and M. A. Khayat, "Issues and methods concerning the evaluation of hypersingular and near-hypersingular integrals in BEM formulations," presented at the Int. Conf. on Electromagnetics in Advanced Applications (ICEAA), Turin, Italy, Sep. 12–16, 2005.

Implementation of Method of Moments for Numerical Analysis of Corrugated Surfaces With Impedance Boundary Condition

Ilari Hänninen and Keijo Nikoskinen

***Abstract*—A method of moments formulation is developed to analyze the scattering of corrugated surfaces by using an impedance boundary condition. The numerical analysis of the impedance surface is done using closed-form formulae and accurate numerical integration. The studied formulation greatly decreases the computational resources required to study corrugated structures.**

***Index Terms*—Corrugated surface, method of moments (MoM), radar cross section (RCS).**

I. INTRODUCTION

Corrugated surfaces pose challenging problems regarding numerical computations. They are constructed—in terms of wavelength—of very thin grooves, that require a very fine mesh to model, which in turn leads to high memory requirements and long computation times. On the other hand, corrugation is usually used in situations where the corrugation is quite uniform and continuous on a relatively large surface area. Thus the small-scale effects on the scattering response of the individual grooves are usually masked by the large-scale effects of the corrugated surface as a whole. If one were able to replace the corrugation in the numerical model by a surface that has the same large-scale effects as the corrugated surface but which is smooth, i.e., without grooves, one could diminish the high computational cost considerably.

Manuscript received February 2, 2007; revised September 1, 2007.

The authors are with the Electromagnetics Laboratory, Helsinki University of Technology, FI-02150 Espoo, Finland (e-mail: ilari.hanninen@tkk.fi).

Digital Object Identifier 10.1109/TAP.2007.913171

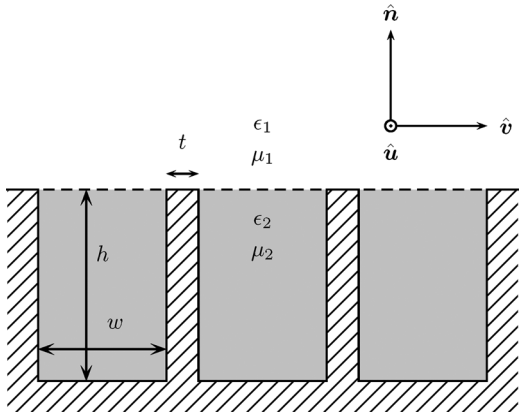

Fig. 1. Geometry and the physical properties of the corrugation.

In this Communication, the authors introduce a method of moments (MoM) implementation which exploits the impedance boundary condition (IBC) in numerical analysis of the corrugation. The method proposed treats the grooves of the corrugation as short-circuited waveguides, which enables one to compute the impedance values analytically. Previously, a method applying the soft-and-hard surface (SHS) [1], [2] boundary approximation was suggested for the computational analysis of corrugated surfaces [3]. However, the SHS approximation is valid only for a single frequency whereas the IBC can be used to compute the scattering response of the corrugated surface for a frequency band around and including the SHS case. Asymptotic boundary conditions (ABC) have also been used to model corrugations with good success [4]–[6]. The IBC method was chosen in this paper because it is simple, easy to implement, and reduces the number of unknowns significantly. The IBC is used with a surface integral equation method to solve the scattered field numerically, using MoM. The results produced by this method are compared to the numerical analysis of the exact model of the corrugation by *CST Microwave Studio* using finite integration technique (FIT).

II. IMPEDANCE BOUNDARY CONDITION FOR CORRUGATED SURFACE

Let us consider a corrugated surface that is sufficiently smooth so that it can be locally approximated by a flat surface. We will denote the direction of the corrugation by $\boldsymbol{u}$ and the direction perpendicular to the corrugation by $\boldsymbol{v}$, so that $\boldsymbol{u} \times \boldsymbol{v} = \boldsymbol{n}$, where $\boldsymbol{n}$ is the unit normal vector to the surface (see Fig. 1). A corrugated surface can be approximated, within certain limitations, by the impedance boundary condition

$$\boldsymbol{E}_t(\boldsymbol{r}) = \overline{\boldsymbol{Z}}_s \cdot \boldsymbol{n}(\boldsymbol{r}) \times \boldsymbol{H}_t(\boldsymbol{r}) \tag{1}$$

where $\boldsymbol{E}_t$ and $\boldsymbol{H}_t$ are the field components tangential to the surface, and $\overline{\boldsymbol{Z}}_s$ is the surface impedance dyadic

$$\overline{\boldsymbol{Z}}_s = Z_u \boldsymbol{u}\boldsymbol{u} + Z_v \boldsymbol{v}\boldsymbol{v}. \tag{2}$$

We can also write the impedance boundary condition by means of the surface admittance dyadic $\overline{\boldsymbol{A}}_s = \overline{\boldsymbol{Z}}_s^{-1}$ as

$$\boldsymbol{H}_t(\boldsymbol{r}) = -\overline{\boldsymbol{A}}_s \cdot \boldsymbol{n}(\boldsymbol{r}) \times \boldsymbol{E}_t(\boldsymbol{r}). \tag{3}$$

The impedance values Z_u and Z_v in (2) can be computed by approximating the grooves of the corrugation by short-circuited wave guides if the width of the grooves is sufficiently small, and the values are given by [3]

$$Z_u = iZ^{\mathrm{TE}_1} \tan(\beta^{\mathrm{TE}_1} h), \quad Z_v = i\eta_2 \tan(k_{2n} h) \tag{4}$$

where $Z^{\mathrm{TE}_1} = \omega\mu_2/\beta^{\mathrm{TE}_1}$ is the wave impedance for the TE_1-waveform, β^{TE_1} is the propagation factor, $k_2 = |\boldsymbol{k}_2|$ and μ_2 are the wave number and permeability inside the corrugation, and $k_{2n} = |\boldsymbol{n} \cdot \boldsymbol{k}_2|$. The impedance component Z_u approaches zero as $k_2 w$ goes to zero, i.e., when the width w of the grooves becomes very small compared to the wavelength. If the incident frequency matches the height of the corrugation h, i.e., incident frequency is at the resonant frequency of the structure, the impedance component Z_v is infinite. At the resonant frequency and for very small groove widths w, so that $Z_u \approx 0$ and $Z_v = \infty$, the corrugated surface may be approximated by the soft and hard surface (SHS), whose boundary condition is

$$\boldsymbol{u}(\boldsymbol{r}) \cdot \boldsymbol{E}(\boldsymbol{r}) = 0, \quad \boldsymbol{u}(\boldsymbol{r}) \cdot \boldsymbol{H}(\boldsymbol{r}) = 0. \tag{5}$$

The SHS boundary condition (5) was previously used to model the scattering behavior of a corrugated surface [3]. However, the SHS boundary condition is not suitable for modeling a corrugated surface that is not at the resonant case, since the impedance values change rapidly if the frequency does not coincide with the resonant case. Also, neither the impedance boundary condition (1) nor the admittance boundary condition (3) alone can be used, since one of the impedance or admittance components is always very large if the incident frequency is close to the resonant frequency, and the numerical computations would then be very inaccurate. When we consider what happens at the limit when we approach the resonant frequency, we should get at the resonant limit the (5). Combining the (1) and (3) then gives us the boundary condition for the impedance surface near the resonant frequency

$$\boldsymbol{u} \cdot \boldsymbol{E} = -Z_u \boldsymbol{v} \cdot \boldsymbol{H}, \quad \boldsymbol{u} \cdot \boldsymbol{H} = \frac{1}{Z_v} \boldsymbol{v} \cdot \boldsymbol{E}. \tag{6}$$

The closer we are to the resonant frequency, the larger the imbalance between the surface current $\boldsymbol{u}$- and $\boldsymbol{v}$-components becomes. Thus, in the numerical computations we replace the small $\boldsymbol{v}$-components of the surface currents $\boldsymbol{J}(\boldsymbol{r}) = \boldsymbol{n}(\boldsymbol{r}) \times \boldsymbol{H}(\boldsymbol{r})$ and $\boldsymbol{M}(\boldsymbol{r}) = -\boldsymbol{n}(\boldsymbol{r}) \times \boldsymbol{E}(\boldsymbol{r})$ by the corresponding $\boldsymbol{u}$-components, as computed from (6)

$$\begin{aligned} \boldsymbol{J}(\boldsymbol{r}) &= \boldsymbol{u}(\boldsymbol{r}) J_u(\boldsymbol{r}) + \boldsymbol{v}(\boldsymbol{r}) J_v(\boldsymbol{r}) \\ &= \boldsymbol{u}(\boldsymbol{r}) J_u(\boldsymbol{r}) + \frac{1}{Z_v} \boldsymbol{v}(\boldsymbol{r}) M_u(\boldsymbol{r}) \end{aligned} \tag{7}$$

$$\begin{aligned} \boldsymbol{M}(\boldsymbol{r}) &= \boldsymbol{u}(\boldsymbol{r}) M_u(\boldsymbol{r}) + \boldsymbol{v}(\boldsymbol{r}) M_v(\boldsymbol{r}) \\ &= \boldsymbol{u}(\boldsymbol{r}) M_u(\boldsymbol{r}) - Z_u \boldsymbol{v}(\boldsymbol{r}) J_u(\boldsymbol{r}). \end{aligned} \tag{8}$$

In practical use this means that in the numerical computations the configuration of the basis functions must be such that they only allow current flow to the $\boldsymbol{u}$-direction on the corrugated surfaces. Another limit that the use of the impedance boundary condition imposes is that the impedance and the admittance values attached to them can not be very large. Thus, the geometrical properties of the corrugation must be close to the resonant case, i.e., the height of the grooves h can not differ too much from the value computed for the SHS-case [1], the width of the grooves w must be small compared to the wavelength, e.g., of order $w \approx \lambda/10$ or smaller, and the thickness of the walls of the grooves t must be smaller than the width of the grooves w, i.e., $t \ll w$. The use of the impedance formulae (4) to model a corrugated surface has been studied for 2-D-structures [7], [8].

III. Surface Integral Equations for the Impedance Surface

The total electric and magnetic field can be written as a sum of the primary (i.e., incident) field and the scattered field

$$\boldsymbol{E}(\boldsymbol{r}) = \boldsymbol{E}^p(\boldsymbol{r}) + \boldsymbol{E}^s(\boldsymbol{r}), \quad \boldsymbol{H}(\boldsymbol{r}) = \boldsymbol{H}^p(\boldsymbol{r}) + \boldsymbol{H}^s(\boldsymbol{r}). \tag{9}$$

The boundary conditions for the impedance surface can now be written as

$$\boldsymbol{u}(\boldsymbol{r}) \cdot (\boldsymbol{E}^p(\boldsymbol{r}) + \boldsymbol{E}^s(\boldsymbol{r})) = Z_u \boldsymbol{u}(\boldsymbol{r}) \cdot \boldsymbol{J}(\boldsymbol{r}) \tag{10}$$

$$\boldsymbol{u}(\boldsymbol{r}) \cdot (\boldsymbol{H}^p(\boldsymbol{r}) + \boldsymbol{H}^s(\boldsymbol{r})) = \frac{1}{Z_v} \boldsymbol{u}(\boldsymbol{r}) \cdot \boldsymbol{M}(\boldsymbol{r}) \tag{11}$$

By using the equivalent surface principle, the boundary conditions (10) and (11), and the (7) and (8), we can in the usual way derive the electric and magnetic field equations for a closed corrugated surface as

$$\begin{aligned} \boldsymbol{u}(\boldsymbol{r}) \cdot \boldsymbol{E}^p(\boldsymbol{r}) = {} & \frac{Z_u}{2} J_u(\boldsymbol{r}) + \frac{1}{i\omega\epsilon_1} \boldsymbol{u}(\boldsymbol{r}) \cdot D(\boldsymbol{u} J_u)(\boldsymbol{r}) + \frac{1}{i\omega\epsilon_1 Z_v} \boldsymbol{u}(\boldsymbol{r}) \\ & \cdot D(\boldsymbol{v} M_u)(\boldsymbol{r}) + \boldsymbol{u}(\boldsymbol{r}) \cdot K(\boldsymbol{u} M_u)(\boldsymbol{r}) - Z_u \boldsymbol{u}(\boldsymbol{r}) \cdot K(\boldsymbol{v} J_u)(\boldsymbol{r}) \end{aligned} \tag{12}$$

and

$$\begin{aligned} \boldsymbol{u}(\boldsymbol{r}) \cdot \boldsymbol{H}^p(\boldsymbol{r}) = {} & \frac{1}{2Z_v} M_u(\boldsymbol{r}) + \frac{1}{i\omega\mu_1} \boldsymbol{u}(\boldsymbol{r}) \cdot D(\boldsymbol{u} M_u)(\boldsymbol{r}) - \frac{Z_u}{i\omega\mu_1} \boldsymbol{u}(\boldsymbol{r}) \\ & \cdot D(\boldsymbol{v} J_u)(\boldsymbol{r}) - \boldsymbol{u}(\boldsymbol{r}) \cdot K(\boldsymbol{u} J_u)(\boldsymbol{r}) - \frac{1}{Z_v} \boldsymbol{u}(\boldsymbol{r}) \cdot K(\boldsymbol{v} M_u)(\boldsymbol{r}) \end{aligned} \tag{13}$$

with the integral operators $K(\boldsymbol{F})(\boldsymbol{r})$ and $D(\boldsymbol{F})(\boldsymbol{r})$ defined as

$$K(\boldsymbol{F})(\boldsymbol{r}) = \left[\int_S \nabla G(\boldsymbol{r}, \boldsymbol{r}') \times \boldsymbol{F}(\boldsymbol{r}') dS' \right]_{\tan} \tag{14}$$

and

$$\begin{aligned} D(\boldsymbol{F})(\boldsymbol{r}) = \Bigg[& p.v. \nabla \int_S G(\boldsymbol{r}, \boldsymbol{r}') \nabla' \cdot \boldsymbol{F}(\boldsymbol{r}') dS' \\ & + k^2 \int_S G(\boldsymbol{r}, \boldsymbol{r}') \boldsymbol{F}(\boldsymbol{r}') dS' \Bigg]_{\tan} \end{aligned} \tag{15}$$

for the closed surface S of a volume D and a continuous field $\boldsymbol{F}(\boldsymbol{r})$ tangential to S. The surface integral equations for the SHS used in [3] can be obtained from (12) and (13) by letting $Z_u \to 0$ and $Z_v \to \infty$.

From (12) and (13) the surface currents $J_u(\boldsymbol{r})$ and $M_u(\boldsymbol{r})$ can be solved using MoM. From these, the surface current components $J_v(\boldsymbol{r})$ and $M_v(\boldsymbol{r})$ can be straightforwardly computed by (7) and (8). The basis functions in the MoM formulation must be chosen in such a way that on the general corrugated surface they only allow current flow to the $\boldsymbol{u}$-direction. We have used the rooftop-functions as the basis and the testing functions in the numerical computations, as they are the most obvious choice.

IV. Numerical Tests

As a test object, a corrugated plate of size $3\lambda \times 3\lambda \times 0.3\lambda$ (width $\times$ length $\times$ height) was used, with incident frequency $f = 1$ GHz. The groove height h of the corrugation varied from 0.19λ to 0.25λ in 0.02λ steps, and the groove widths w used were 0.05λ, 0.08λ, 0.10λ and 0.125λ. This relatively simple object was chosen in order to minimize the effects of a more complicated geometry to the scattering results; the effect of the corrugation and its physical properties to the scattering properties are more easily studied when these effects can be readily compared with the scattering response of the corresponding perfect electric conductor (PEC) plate. Closed-form formulae and accurate numerical integration were used to compute the singular integrals in the MoM equations [9], [10]. Since the computation of the scattering response of corrugated surfaces poses several problems for the surface integral methods (the mesh size required to accurately model the corrugation leads to very large system matrix sizes, i.e., very high memory requirements and long computation times, the surface elements need to be very small compared to the wavelength which may lead the so-called

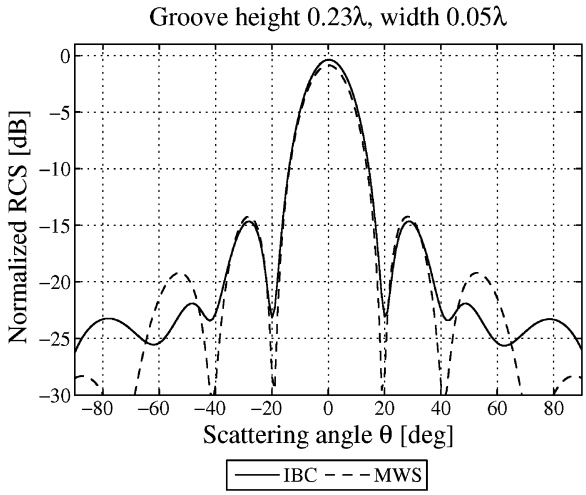

Fig. 2. Normalized co-polar RCS for incident angle $\theta = 0$, $\varphi = 0$, and for corrugation height $h = 0.23\lambda$ and width $w = 0.05\lambda$.

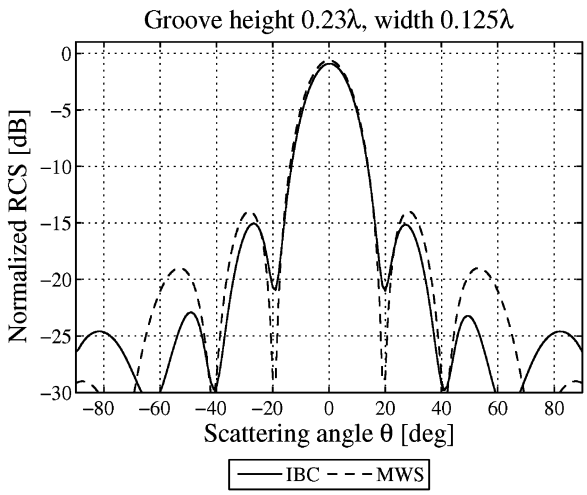

Fig. 3. Normalized co-polar RCS for incident angle $\theta = 0$, $\varphi = 0$, and for corrugation height $h = 0.23\lambda$ and width $w = 0.125\lambda$.

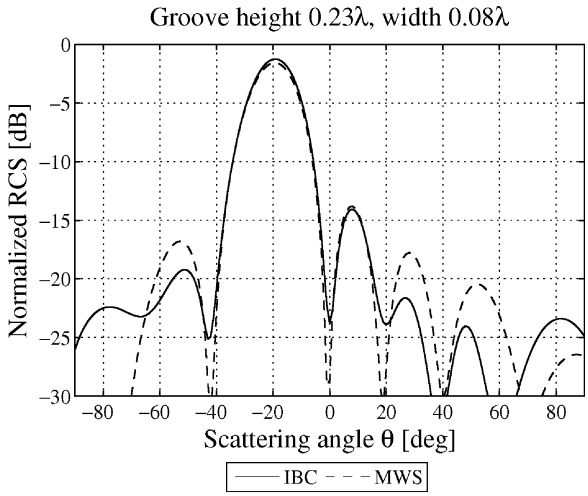

Fig. 4. Normalized co-polar RCS for incident angle $\theta = 20$, $\varphi = 0$, and for corrugation height $h = 0.23\lambda$ and width $w = 0.08\lambda$.

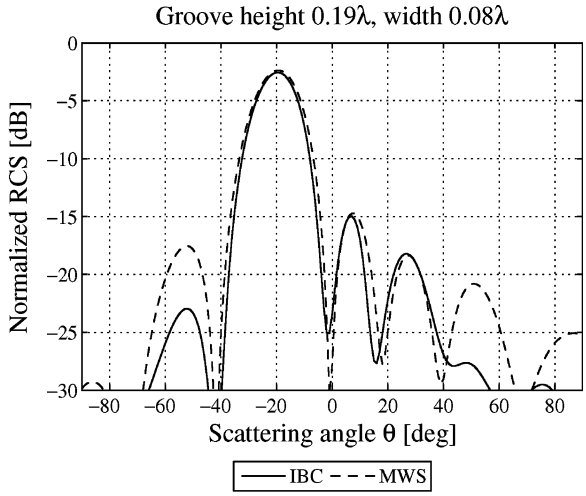

Fig. 5. Normalized co-polar RCS for incident angle $\theta = 20$, $\varphi = 0$, and for corrugation height $h = 0.19\lambda$ and width $w = 0.08\lambda$.

sub-wavelength breakdown), we chose to compare the IBC method results to the results obtained by *CST Microwave Studio* (MWS), which uses finite integration technique (FIT). The *CST Microwave Studio* was chosen for reference since the geometry of the problem is ideally suited to the FIT grid, and the computation times of the FIT method are relatively short compared to the surface integral methods. For MWS, the thickness of the walls between the grooves was chosen as $t = 0.01\lambda$.

The quantities compared were the bistatic co-polar radar cross sections (RCSs) computed by the impedance boundary condition method and by MWS. The results were normalized so that the 0 dB level corresponds to the maximum RCS value of the corresponding smooth PEC plate for normal incidence. Since near the resonant frequency the corrugated plate the co-polar response is dominant, we show only the co-polar RCSs as the strength of the scattered cross-polarized field is too small to have any significance in the results. The scattering responses were computed in 10° steps for incident angles $\theta = [0^\circ, 50^\circ]$, measured from the normal direction, and for incident angles $\varphi = 0^\circ$, $\varphi = 90^\circ$, measured from the u-axis towards the v-axis, with $\varphi = 0^\circ$ coinciding with the direction of the corrugation. The incident angle $\varphi = 0^\circ$ is the most troublesome direction regarding the accuracy of the impedance values obtained from (4), since the angular dependency of the impedance values is greatest when the incident wave is propagating to the direction of the corrugation. Thus, for sideward incidence, we show the scattering results for this angle, since it is the most interesting direction. For corrugations that are not filled with any dielectric material, as is the case here, the groove height $h_{\text{res}} = 0.25\lambda$ corresponds to the resonant frequency. Since the impedance values given by (4) are the same for $h = h_{\text{res}} \pm x$, the IBC results for the groove heights given above are also valid for values of h that are larger than 0.25λ by a similar factor. This was verified by computing the scattering response for the corresponding groove heights using MWS and comparing them with the results for the values given above. The incident field was left-handedly circularly polarized in all cases. Due to practical constraints, the sides of the MWS model of the corrugated plate were left open, whereas for the impedance boundary condition method (IBC) the side surfaces in the model were smooth. Thus for scattering angles close to the tangent plane of the corrugated surface, this difference may explain the slightly different results for the scattering fields computed by the two methods.

Figs. 2 and 3, show the RCSs for normal incidence for groove height $h = 0.23\lambda$, and for groove widths $w = 0.05\lambda$ and $w = 0.125\lambda$. Figs. 4 and 5 show the RCSs for incident angles $\theta = 20^\circ$, $\varphi = 0^\circ$, for groove

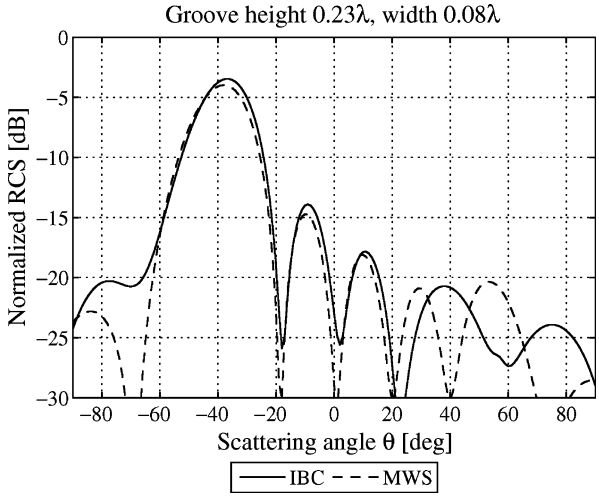

Fig. 6. Normalized co-polar RCS for incident angle $\theta = 40$, $\varphi = 0$, and for corrugation height $h = 0.23\lambda$ and width $w = 0.08\lambda$.

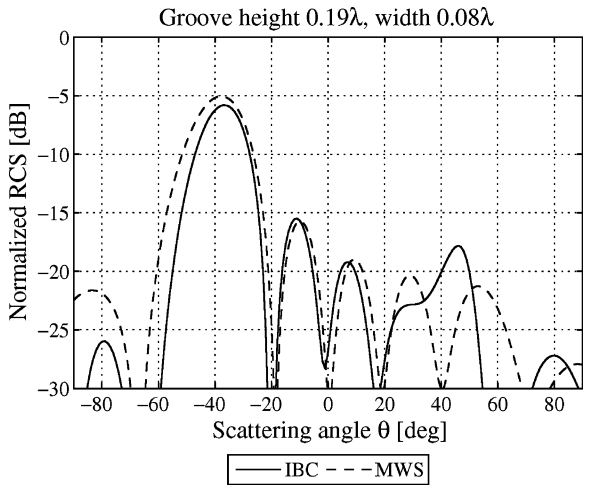

Fig. 7. Normalized co-polar RCS for incident angle $\theta = 40$, $\varphi = 0$, and for corrugation height $h = 0.19\lambda$ and width $w = 0.08\lambda$.

width $w = 0.08\lambda$, and for groove heights $h = 0.23\lambda$ and $h = 0.19\lambda$, and Figs. 6 and 7 show RCSs for incident angles $\theta = 40^\circ$, $\varphi = 0^\circ$, for groove width $w = 0.08\lambda$, and for groove heights $h = 0.23\lambda$ and $h = 0.19\lambda$. As can be seen from the figures, the IBC results generally agree well with the MWS results to the direction of the main beam and the first side beams. Further observations show that to the scattering directions close to tangent plane of the corrugated plate, the IBC results show some fluctuations that do not agree with the MWS results, although the RCS values for these directions are quite small so the comparison is difficult. Similarly, for incident angle $\theta = 40^\circ$, and especially for groove height $h = 0.19\lambda$, the IBC and MWS results start to differ slightly. These differences are somewhat expected, since the impedance boundary condition can not be presumed to properly model the corrugated plate in the sideward directions due to the angular dependency of the impedance values. Also, for groove width $w = 0.125\lambda$ the differences in the results are somewhat larger than for groove width $w = 0.05\lambda$, especially in the side beams. This is an indication that the groove width can not be much larger than 0.1λ, since for larger values the assumptions made in the impedance value analysis no longer stand.

Due to the various parameters affecting the accuracy of the computations, it is difficult to give clear-cut bounds for the applicability of the IBC method. In the light of the numerical results, it seems that the following limits are reasonable: the width of the grooves should be $w \leq 0.1\lambda$, the height of the grooves $0.19\lambda \leq h \leq 0.31\lambda$ (for grooves not filled with a dielectric material), and the incident angle $\theta \leq 40^\circ$.

V. Conclusions

A Method of Moments formulation using an impedance boundary condition has been developed to analyze the scattering properties of corrugated surfaces for a frequency band around and including the resonant frequency, for which the corrugated surface approximates a soft-and-hard surface. The method introduced in this paper offers an efficient and fast numerical method to analyze the scattering properties of corrugated surfaces near the resonant frequency. The results obtained by the method have been verified using *CST Microwave Studio*.

Acknowledgment

The authors would like to thank I. Laakso of the Electromagnetics Laboratory, Helsinki University of Technology, for his help in computing the *CST Microwave Studio* results.

References

[1] P.-S. Kildal, "Artificially soft and hard surfaces in electromagnetics," *IEEE Trans. Antennas Propag.*, vol. 38, no. 10, pp. 1537–1544, Oct. 1990.

[2] I. V. Lindell, "Generalized soft-and-hard surface," *IEEE Trans. Antennas Propag.*, vol. 50, no. 7, pp. 926–929, Jul. 2002.

[3] I. Hänninen, M. Pitkonen, K. I. Nikoskinen, and J. Sarvas, "Method of moments analysis of the backscattering properties of a corrugated trihedral corner reflector," *IEEE Trans. Antennas Propag.*, vol. 54, no. 4, pp. 1167–1173, Apr. 2006.

[4] Z. Sipus, H. Merkel, and P.-S. Kildal, "Green's functions for planar soft and hard surfaces derived by asymptotic boundary conditions," *Proc. Inst. Elect. Eng. Microw. Antennas Propag.*, vol. 144, no. 5, pp. 321–328, Oct. 1997.

[5] A. A. Kishk, "Analysis of hard surfaces of cylindrical structures of arbitrarily shaped cross section using asymptotic boundary conditions," *IEEE Trans. Antennas Propag.*, vol. 51, no. 6, pp. 1150–1156, Jun. 2003.

[6] A. A. Kishk, "Electromagnetic scattering from transversely corrugated cylindrical structures using the asymptotic corrugated boundary conditions," *IEEE Trans. Antennas Propag.*, vol. 52, no. 11, pp. 3104–3108, Nov. 2004.

[7] A. A. Kishk and P.-S. Kildal, "Electromagnetic scattering from two dimensional anisotropic impedance object under oblique plane wave incidence," *ACES J.*, vol. 10, no. 3, pp. 81–92, 1995.

[8] T. M. Uusitupa, "Usability studies on approximate corrugation models in scattering analysis," *IEEE Trans. Antennas Propag.*, vol. 54, no. 9, pp. 2486–2496, Sep. 2006.

[9] P. Ylä-Oijala and M. Taskinen, "Calculation of CFIE impedance matrix elements With RWG and $n\times$, RWG functions," *IEEE Trans. Antennas Propag.*, vol. 51, no. 8, pp. 1837–1846, Aug. 2003.

[10] I. Hänninen, M. Taskinen, and J. Sarvas, "Singularity subtraction integral formulae for surface integral equations with Rwg, rooftop and hybrid basis functions," *Progr. Electromagn. Res.*, vol. 63, pp. 243–278, 2006.